Supporting Information

Novel methotrexate prodrug-targeted drug delivery system based on PEG-lipid-PLA hybrid nanoparticles for enhanced anticancer efficacy and reduced toxicity of mytomycin C

Yang Li, [ac] Jinyan Lin, [a] Hongjie Wu, [b] Mengmeng Jia, [a] Conghui Yuan, [a] Ying Chang, [a] Zhenqing Hou, [a,*] Lizong Dai [a,*]

[a] College of Materials, Xiamen University, Xiamen 361005, China

[b] Department of Pharmacy, College of Pharmacy, Xiamen University, Xiamen 361005, China

[c] Department of Chemistry, College of Chemistry & Chemical Engineering, Xiamen University, Xiamen 361005, China

* Corresponding authors.

E-mail addresses: lzdai@xmu.edu.cn (L. Dai), houzhenqing@xmu.edu.cn (Z. Hou),

Tel. +86-592-2186178.

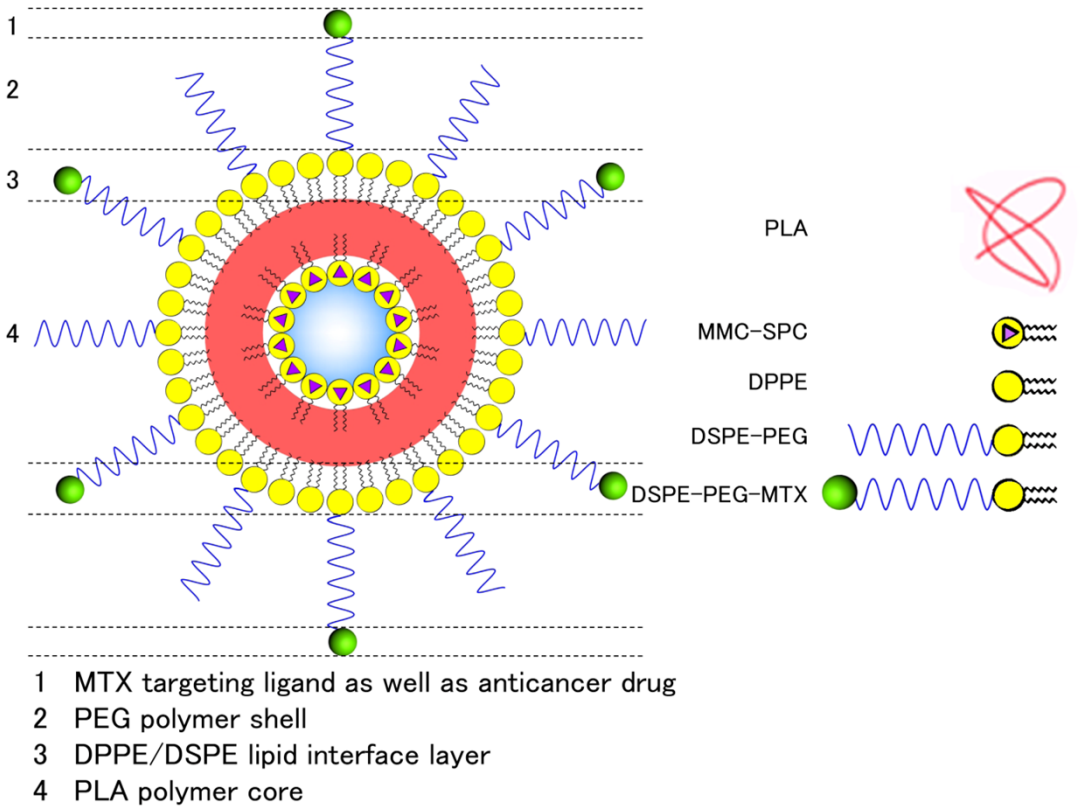

Fig. S1† More details of schematic illustration of the MTX-PEG-PE-PLA NPs/MMC-SPC comprised of a PLA hydrophobic core loaded with MMC-SPC, an amphiphilic PE interface layer, a hydrophilic PEG shell with a targeting ligand MTX on the surface.

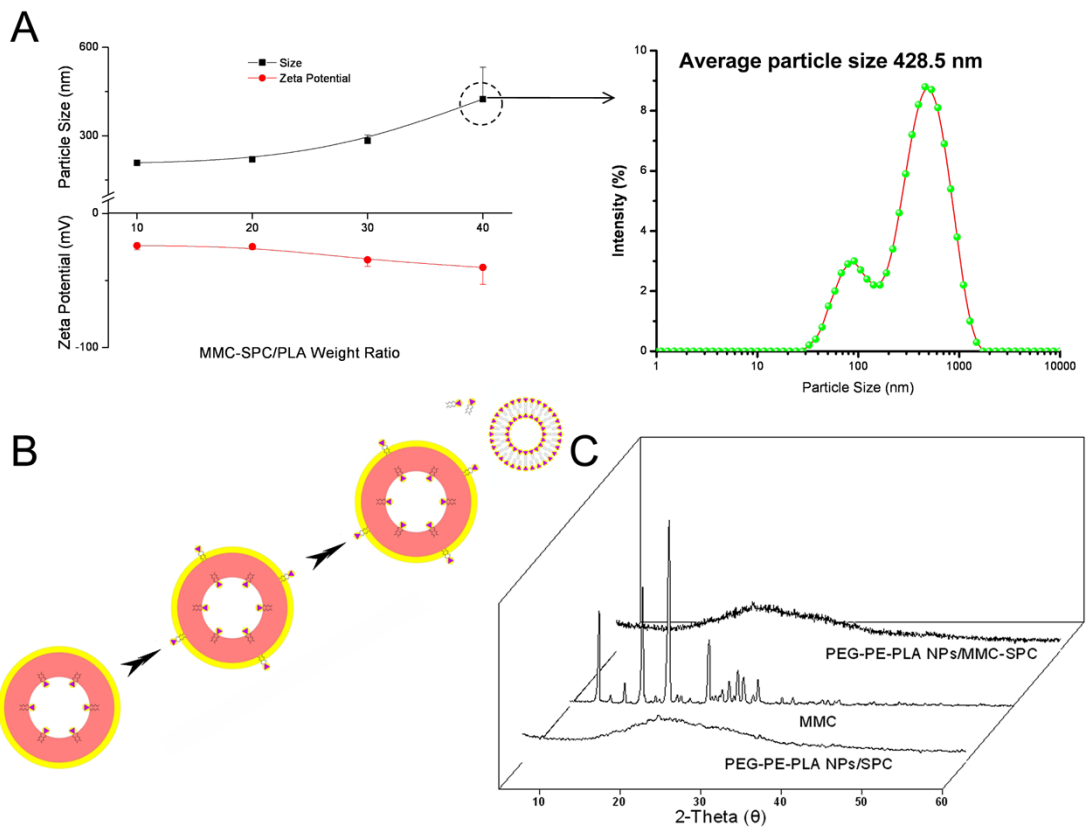

Fig. S2† (A) The key characteristics of the MTX-PEG-PE-PLA NPs/MMC-SPC prepared with a series of MMC-SPC/PLA polymer weight ratios: particle size and zeta potential. The arrowhead indicated the particle size and particle size distribution of the MTX-PEG-PE-PLA NPs/MMC-SPC (MMC-SPC/PLA polymer weight ratio = 40%). (B) Model of the MMC-SPC-loaded MTX-PEG-PE-PLA NPs prepared with a series of MMC-SPC/PLA polymer weight ratios. (C) XRD analysis of the PEG-PE-PLA NPs/MMC-SPC. The XRD peak of MMC was absent in the PEG-PE-PLA NPs/MMC-SPC, indicating that MMC drug in the hybrid PEG-PE-PLA NPs was present in either molecular dispersion or amorphous state.

	Particle Size	Polydispersity (PDI)	Zeta potential	Encapsulation efficiency (%)
PEG-PE-PLA NPs/MMC-SPC	201.2±2.5	0.129±0.030	-27.93±3.46	90.6±2.3
MTX-PEG-PE-PLA NPs/MMC-SPC	219.6±2.1	0.187±0.021	-24.76±2.71	90.5±3.0

Table S1† Physicochemical characterization of the PEG-PE-PLA NPs/MMC-SPC and MTX-PEG-PE-PLA NPs/MMC-SPC: particle size, PDI, zeta potential and drug encapsulation efficiency (mean ± SD, n=3).

The particle size and zeta potential of the MTX-PEG-PE-PLA NPs/MMC-SPC increased over those of the PEG-PE-PLA NPs/MMC-SPC, which was predominately related to the presence of MTX.

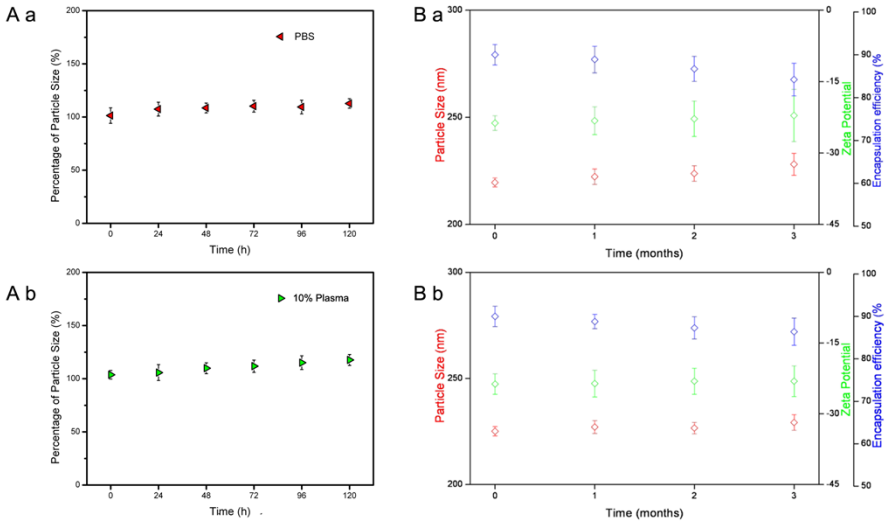

Fig. S3† (A) In vitro short-term stability of the MTX-PEG-PC-PLA NPs/MMC-SPC in PBS or 10% plasma for 120 h (mean ± SD, n=3). (B) In vitro long-term stability of the MTX-PEG-PE-PLA NPs/MMC-SPC at (a) 4 or (b) 25°C (mean ± SD, n=7).

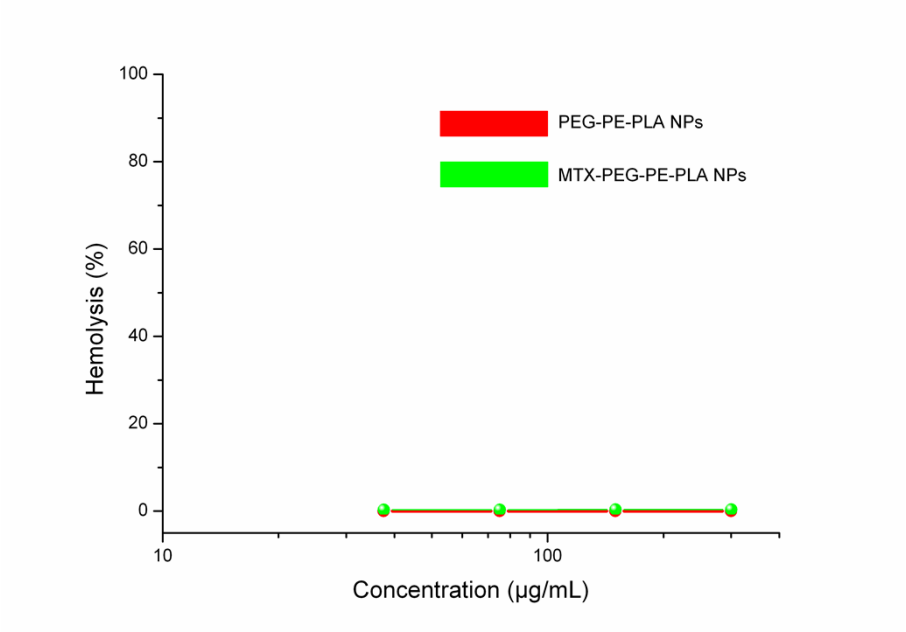

Fig. S4† Hemolysis assay of the MMC drug-free NPs such as the PEG-PE-PLA NPs or MTX-PEG-PE-PLA NPs at different concentrations (37.5, 75, 150 and 300 μg/ml of PBS) using water as a positive control and PBS as a negative control.

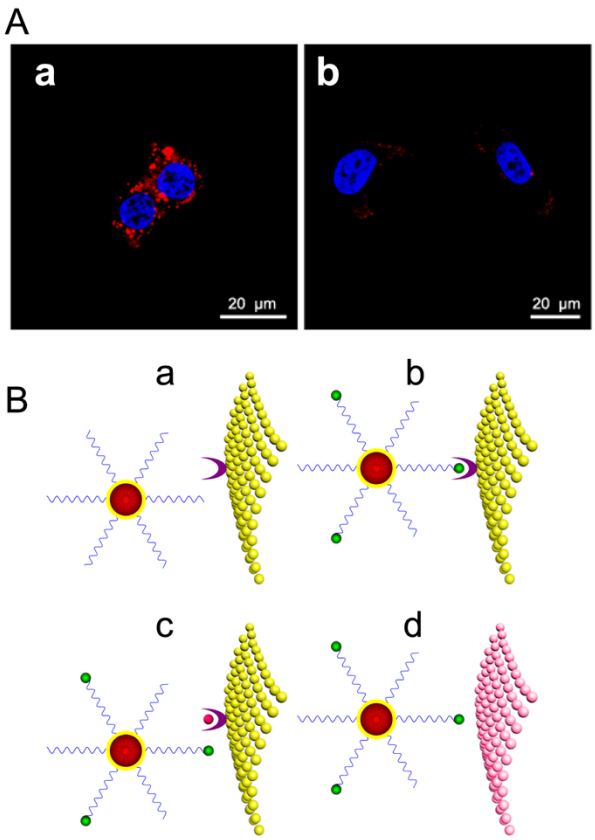

Fig. S5† (A) In vitro cellular uptake of the MTX-PEG-PE-PLA NPs/MMC-SPC/DiD. (a) FA receptor-positive Caco-2 cells or (b) FA receptor-negative MC 3T3-E1 cells were treated with the MTX-PEG-PE-PLA NPs/MMC-SPC/DiD for 6 h, and then observed by LCSM. (B) More details of illustration of the cell uptake pathway of the PEG-PE-PLA NPs/MMC-SPC and MTX-PEG-PE-PLA NPs/MMC-SPC. (a) The PEG-PE-PLA NPs/MMC-SPC entered the FA receptor-positive cells such as HeLa cells by the carriers mediated endocytosis or phagocytosis. (b) The MTX-PEG-PE-PLA NPs/MMC-SPC entered the FA receptor-positive cells such as HeLa cells by the FA receptor mediated endocytosis. (c) When the FA receptor-positive cells such as HeLa cells were pre-incubated with the MTX-PEG-PE-PLA NPs/MMC-SPC in the presence of an excess of the free FA, the increased intracellular internalization of NPs was drastically blocked as a result of no availability of FA receptor on the surface of the cells. (d) The MTX-PEG-PE-PLA NPs/MMC-SPC entered the FA receptor-negative cells such as A549 cells by the carriers mediated endocytosis or phagocytosis.

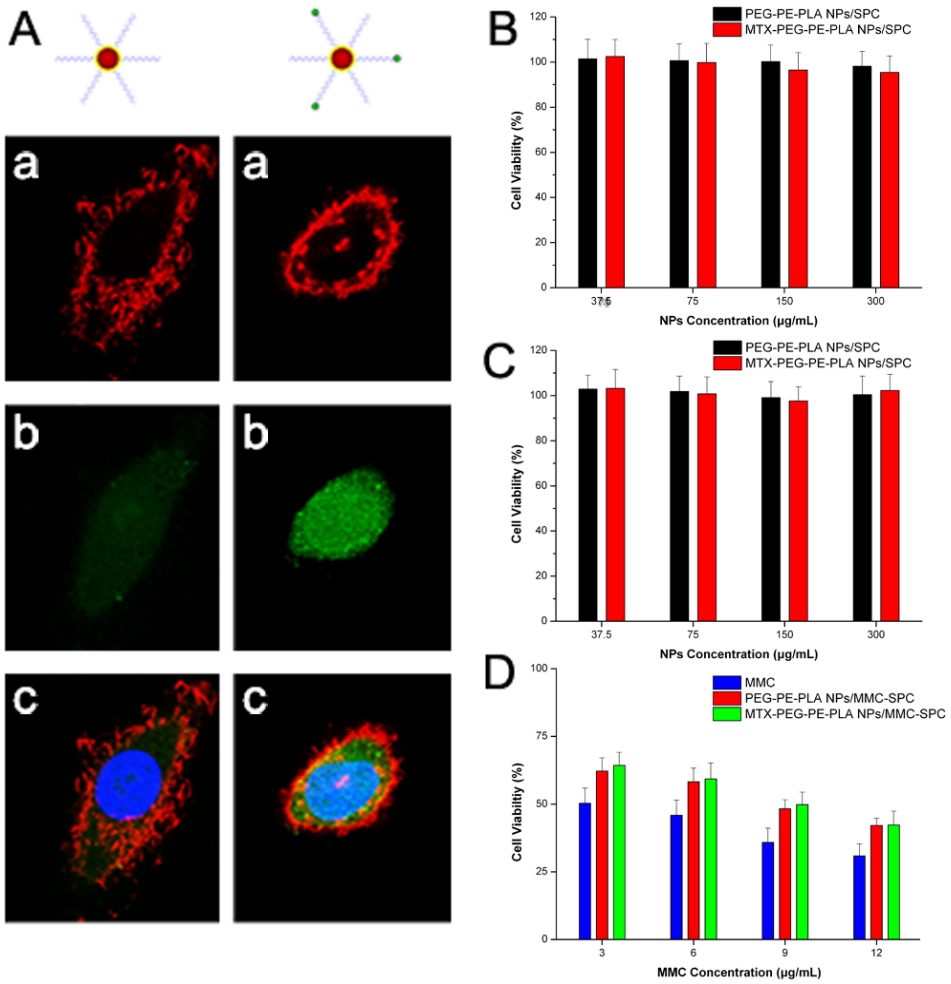

Fig. S6† (A) LCSM images of HeLa cells after incubation with the PEG-PE-PLA NPs/FITC-MMC-SPC or MTX-PEG-PE-PLA NPs/FITC-MMC-SPC for 12 h. (a) were the rhodamine phalloidin channel showing red fluorescence. (b) were the FITC channel which showing green fluorescence. The overlap of the images in (a) and (b) was shown in (c). The nuclei were stained with Hoechst 33258 (blue). (B) Cell viability of the PEG-PE-PLA NPs/SPC and MTX-PEG-PE-PLA NPs/ SPC against HeLa cells after incubation for 24 h (mean ± SD, n = 6). (C) Cell viability of the PEG-PE-PLA NPs/SPC and MTX-PEG-PE-PLA NPs/ SPC against A549 cells after incubation for 24 h (mean ± SD, n = 6). (D) Cell viability of the PEG-PE-PLA NPs/MMC-SPC and MTX-PEG-PE-PLA NPs/MMC-SPC against A549 cells after incubation for 24 h (mean ± SD, n = 6).

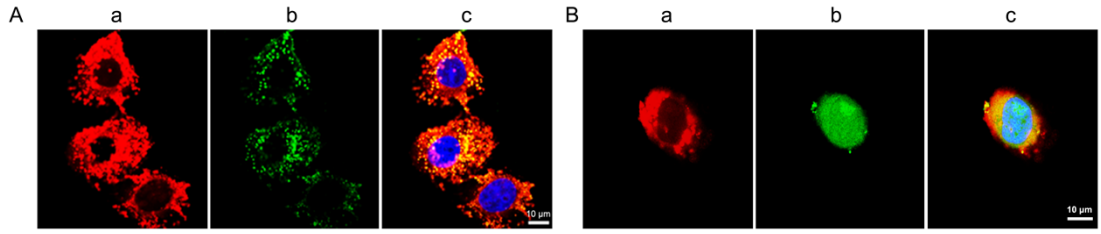

Fig. S7† (A) Subcellular localization of the MTX-PEG-PE-PLA NPs/MMC-SPC/DiD observed by LCSM. Lysosomal colocalization of the MTX-PEG-PE-PLA NPs/MMC-SPC/DiD in HeLa cells after incubation for 8 h was observed by LCSM through (a) the DiD channel and (b) the LysoTracker green channel. The overlap of the images in (a) and (b) was shown in (c). The nuclei were stained with Hoechst 33258 (blue). The MTX-PEG-PE-PLA NPs/MMC-SPC/DiD appeared in red. Lysotracker Green was used to identify endo/lysosomes. (B) LCSM images of HeLa cells after incubation for 12 h with the MTX-PEG-PE-PLA NPs/FITC-MMC-SPC/DiD. (a) was the DiD channel showing red fluorescence from MTX-PEG-PE-PLA NPs/DiD. (b) was the FITC channel showing green fluorescence from FITC-MMC. The overlap of the images in (a) and (b) was shown in (c). The nuclei were stained with Hoechst 33258 (blue).

The intracellular delivery of the MTX-PEG-PE-PLA NPs/FITC-MMC-SPC/DiD was investigated by LCSM. As shown in Figure **S7B†**, the green fluorescence was presented in the cell and the red fluorescence in the cytoplasm. This finding was similar to the reported work. [1] It was also reported that the premature released FITC or FITC-MMC could be not internalized by the cells. [2] To the surprising result, we proposed two possible reasons, one was that the NPs did not finish drug release, thus the one part of drug retained inside the NPs, and the other part of drug released from the NPs and traversed to the perinuclear region. Alternatively, the other was that the high nuclear accumulation of MMC resulted in the subsequent diffusion to other cytoplasmic areas. Regardless of either mechanism, the result confirmed that the drug delivered to the nuclei resulted from the rapid NPs internalization, followed by the efficient intracellular drug release and transport.

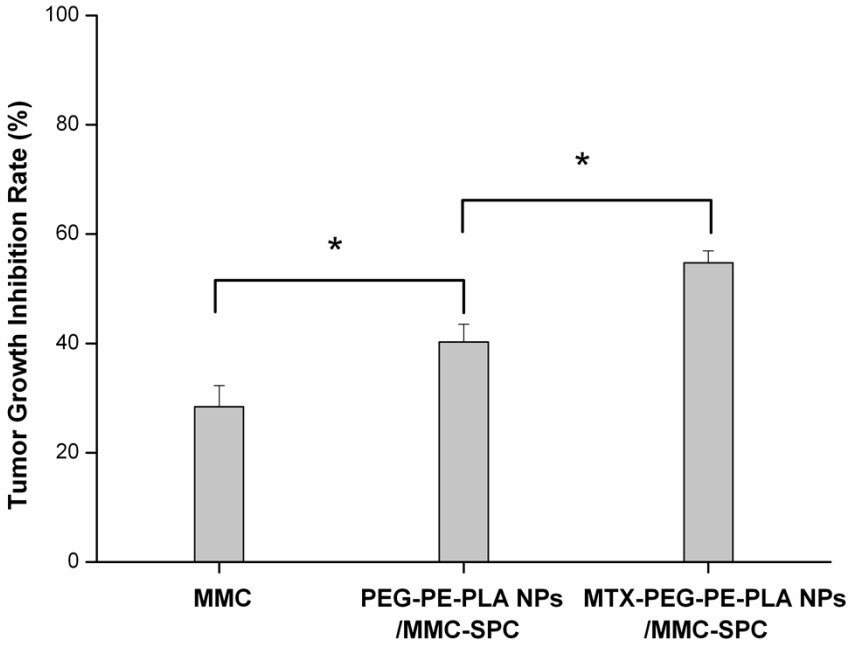

Fig. S8† At the end of experiment (15 d), the mice bearing H_{22} tumor were terminated and the tumors were dissected and weighed. Tumor growth inhibition rate % = (tumor weight of control group - tumor weight of experimental group)/tumor weight of control group × 100% (mean ± SD, n=10). *, $P < 0.05$.

Refrerences

1. S. Han, Y. Liu, X. Nie, Q. Xu, F. Jiao, W. Li, Y. Zhao, Y. Wu and C. Chen, *Small*, 2012, **8**, 1596-1606.
2. H. Wang, Y. Zhao, Y. Wu, Y.-l. Hu, K. Nan, G. Nie and H. Chen, *Biomaterials*, 2011, **32**, 8281-8290.